

# Massively Parallel Finite Volume Computation of Three-dimensional Thermal Convective flows

Ping Wang

Jet Propulsion Laboratory  
California Institute of Technology  
MS 168-522, 4800 Oak Grove Drive  
Pasadena, CA 91109-8099, U.S.A.  
Email: wangpj@rockymt.jpl.nasa.gov

**Abstract-** A parallel implementation of the finite volume method for three-dimensional, time-dependent, thermal convective flows is presented. The algebraic equations resulting from the finite volume discretization are solved by a parallel multigrid method. A flexible parallel code has been implemented on the distributed-memory systems, by using domain decomposition techniques and the MPI communication software. The code uses 1D, 2D, or 3D partitions according to different geometries. It currently runs on the Intel Paragon, the Cray T3D, T3E, the IBM SP2, and the Beowulf system, which can be ported easily to other parallel systems. A comparison of wallclock time of the code among these systems is made, and code performances with respect to different number of processors are presented.

## Nomenclature

|                 |                                     |
|-----------------|-------------------------------------|
| $g$             | acceleration due to gravity         |
| $H$             | height of cavity                    |
| $L$             | length of cavity                    |
| $D$             | width of cavity                     |
| $R$             | Rayleigh number                     |
| $T$             | non-dimensional temperature         |
| $p$             | non-dimensional pressure            |
| $p^*$           | best estimate of pressure           |
| $p'$            | pressure correction                 |
| $x, y, z$       | non-dimensional coordinates         |
| $u, v, w$       | non-dimensional velocity components |
| $u^*, v^*, w^*$ | velocity components based on $p^*$  |
| $u', v', w'$    | velocity corrections                |

## Greek symbols

|          |                                  |
|----------|----------------------------------|
| $\alpha$ | under-relaxation factor          |
| $\beta$  | coefficient of thermal expansion |
| $\kappa$ | thermal diffusivity              |
| $\nu$    | kinematic viscosity              |
| $\sigma$ | Prandtl number                   |

## 1. INTRODUCTION

Thermal Convective motions driven by lateral temperature gradients are important in many areas of interest in industry and in nature. Applications include the temperature control of circuit board components under natural convection

in the electronics industry, heating and ventilation control in building design and construction, cooling systems for nuclear reactors in the nuclear industry, flows and heat transfer associated with all stages of the power generation process, crystal growth procedures, solar-energy collectors in the power industry and atmospheric and fluvial dispersion in the environment.

Due to the wide range of applications, studies of natural convection flow and heat transfer have been pursued vigorously for many years. A typical model of convection driven by a lateral thermal gradient consists of a two or three dimensional cavity with the two vertical end walls held at different constant temperatures. In order to determine the flow structure and heat transfer across cavities with different physical properties, numerous analytical, experimental and computational techniques have been used. In this paper, numerical simulations for thermal Couette flows are discussed. The most numerically studied form of this problem is the case of a rectangular cavity with differentially heated sidewalls. The two dimensional version of this problem has received considerable attention [1] [2] [3] [4] [5], but for the three dimensional case, very few results have been obtained. The first numerical solution of the 3D thermal cavity problem is reported by Mallinson and de Vahl Davis [6], and a numerical study of 3D

natural convection for air in the cubic enclosure is reported in [7] for the Rayleigh number from  $10^3$  to  $10^6$ . For large Rayleigh number 3D flows, there are seldom numerical results available. The existing three dimensional numerical simulations are still in a rudimentary stage. Most existing numerical studies have suffered from insufficient resolution, and the prominent characteristics of complicated three dimensional flows have not been discussed in sufficient depth because the accuracy of the solution is not good enough. In particular, at large Rayleigh numbers, greatly enhanced numerical capabilities are essential in order to catch the significant dynamic features in thin boundary layers. The main reason of these was due to the limitation of computing power and memory size. The significant computational resources of modern, massively parallel supercomputers promise to make such studies feasible. In order to determine such flow structures and heat transfer at large Rayleigh numbers, numerical simulations for the Navier-Stokes equations and the Energy equations are considered on parallel computing systems.

With the development of computer science and numerical analysis, a wide range of powerful numerical methods have been devised for solving fluid dynamical problems and indeed the whole development of numerical methods for approximating partial differential equations has always been influenced and motivated strongly by their application to the equations of fluid dynamics. There has been a trend towards the development of methods specifically for fluid dynamics, and the most widely used methods are those based on either finite difference, finite volume, or finite element. A number of numerical algorithms have been developed for incompressible fluid flows, such as MAC [8], Projection Method [9], and etc. [10]. The SIMPLE algorithm of Patankar and Spalding [11] provided a remarkably successful implicit method, which is used widely in the field of numerical simulations of incompressible flows [12]. This algorithm based on the finite volume formulation lends itself to easy physical interpretation, and it ensures that if conservation is satisfied for each control volume, it is also satisfied for the entire calculation domain. A clear and detailed description of SIMPLE is given by Patankar [13].

In this paper, a numerical study for three dimensional time-dependent problems will be investigated by using massively parallel computing systems, and an efficient numerical scheme and a general and portable parallel implementation will be presented. Section 2 describes the mathematical formulation of the three dimensional,

time dependent thermal cavity flows. Finite volume method and multigrid scheme are given in Section 3. The detailed parallel implementation and the code performance are described in Section 4. The three-dimensional numerical solutions with various Rayleigh numbers up to  $10^7$  are discussed in Section 5. The summary of the present work is given in Section 6.

## 2. MATHEMATICAL FORMULATION

The flow domain is a 3D cavity of  $0 < x < L$ ,  $0 < y < D$ , and  $0 < z < H$ . The appropriate governing equations, subject to the Boussinesq approximation, can be written in non-dimensional form as

$$\frac{\partial u}{\partial x} + \frac{\partial v}{\partial y} + \frac{\partial w}{\partial z} = 0, \quad (1)$$

$$\frac{1}{\sigma} \left( \frac{\partial u}{\partial t} + u \frac{\partial u}{\partial x} + v \frac{\partial u}{\partial y} + w \frac{\partial u}{\partial z} \right) = - \frac{\partial p}{\partial x} + \nabla^2 u, \quad (2)$$

$$\frac{1}{\sigma} \left( \frac{\partial v}{\partial t} + u \frac{\partial v}{\partial x} + v \frac{\partial v}{\partial y} + w \frac{\partial v}{\partial z} \right) = - \frac{\partial p}{\partial y} + \nabla^2 v, \quad (3)$$

$$\frac{1}{\sigma} \left( \frac{\partial w}{\partial t} + u \frac{\partial w}{\partial x} + v \frac{\partial w}{\partial y} + w \frac{\partial w}{\partial z} \right) = - \frac{\partial p}{\partial z} + \nabla^2 w + RT, \quad (4)$$

$$\frac{\partial T}{\partial t} + u \frac{\partial T}{\partial x} + v \frac{\partial T}{\partial y} + w \frac{\partial T}{\partial z} = \nabla^2 T. \quad (5)$$

The dimensionless variables in these equations are the fluid velocities  $u, v, w$ , the temperature  $T$ , and the pressure  $p$ , where  $\sigma = \nu/\kappa$  is the Prandtl number and  $R = g\beta\Delta Th^3/\kappa\nu$  is the Rayleigh number. Here  $\nu$  is the kinematic viscosity,  $\kappa$  is the thermal diffusivity,  $\beta$  is the coefficient of thermal expansion, and  $g$  is the acceleration due to gravity. The rigid end walls on  $x=0, L$  are maintained at constant temperatures  $T_0$  and  $T_0 + \Delta T$  respectively, while the other boundaries are assumed to be insulating. So the boundary conditions on the rigid walls of the cavity are

$$u = v = w = 0 \quad (6)$$

$$\text{on } x = 0, \Gamma, \quad y = 0, D, \quad z = 0, H,$$

$$T = 0 \quad \text{on } x = 0, \quad (7)$$

$$T = 1 \quad \text{on } x = L, \quad (8)$$

$$\frac{\partial T}{\partial z} = 0 \quad \text{on } z = 0, H, \quad (9)$$

$$\frac{\partial T}{\partial y} = 0 \quad \text{on } y = 0, D. \quad (10)$$

In general the motion is controlled by the parameters  $\sigma, R$  and the flow domain.

## 3. NUMERICAL APPROACH

An efficient and practical numerical approach for three dimensional time-dependent thermal

convective flow problems is studied. This implementation is based on the widely used finite volume method (SIMPLE [13]) with an efficient and fast elliptic multigrid scheme for predicting incompressible fluid flows, which proved to be a remarkably successful implicit method. A normal staggered grid configuration is used and the conservation equations are integrated over a macro control volume (Figure 1:  $i$  control volume). Here, velocities are stored at the six surfaces of the control volume marked by  $(u_e, u_n, v_n, v_s, w_t, w_b)$ , and the temperature and pressure are stored at the center of the control volume ( $p_i, T_i$ ). Since the solution of the pressure equation derived from the SIMPLE scheme can represent as much as 80% of the total cost for solving the fluid flow problem [12], it is therefore a high priority to solve for  $p$  in an efficient manner. Here, a multigrid scheme is applied to the discretized equations, which acts as a convergence accelerator and reduces the CPU time significantly for the whole computation. Local, flow-oriented, upwind interpolation functions have been used in the scheme to prevent the possibility of unrealistic oscillatory solutions at high Rayleigh numbers.

A brief summary of the SIMPLE method is outlined here, and details that are omitted here may be found in the original reference [13]. For a guessed pressure field  $p^*$ , the imperfect velocity field  $(u^*, v^*, w^*)$  based on this pressure will result from the solution of the following discretization equations :

$$a_e u_e^* = \sum a_{nb} u_{nb}^* + b + (p_i^* - p_E^*) A_e, \quad (11)$$

$$a_n v_n^* = \sum a_{nb} v_{nb}^* + b + (p_i^* - p_N^*) A_n, \quad (12)$$

$$a_t w_t^* = \sum a_{nb} w_{nb}^* + b + (p_i^* - p_T^*) A_t, \quad (13)$$

where the summation is over the appropriate neighbor points.  $A_e, A_n, A_t$  are the areas of the face of the  $P$  control volume at  $e, n, t$  respectively.  $a_e, a_n, a_t, a_{nb}$  and  $b$  are the coefficients of finite-volume equations. The correct velocity fields are computed by the velocity-correction formula:

$$u_e = u_e^* + \frac{A_e}{a_e} (p_i' - p_E'), \quad (14)$$

$$v_n = v_n^* + \frac{A_n}{a_n} (p_i' - p_N'), \quad (15)$$

$$w_t = w_t^* + \frac{A_t}{a_t} (p_i' - p_T'), \quad (16)$$

and the correct pressure is computed by

$$p = p^* + \alpha_p p'. \quad (17)$$

$\alpha_p$  is an under-relaxation factor for the pressure. In the present case a value of 0.5 is used.  $p'$

will result from the solution of the following discretization equation:

$$a_T p' = \sum a_{nb} p'_{nb} + b, \quad (18)$$

which is derived from the continuity equation (1) and velocity-correction equations (11), (15), and (16). The temperature will be solved by the following discretization equation:

$$a_T T = \sum a_{nb} T_{nb} + b, \quad (19)$$

At each time level, the imperfect velocity field  $(u^*, v^*, w^*)$ , the pressure  $p'$ , and the temperature  $T$  satisfy systems of linear equations (11), (12), (13), (18), and (19), respectively. It is essential to numerically solve these algebraic equations efficiently. To do so, we will employ the multigrid method in our computation since the computational complexity of the multigrid obtaining an approximation up to the discretization accuracy is proportional to the number of unknowns. The main idea of the multigrid is to use the solution on a coarse grid to correct the required solution on a fine grid since an error of wavelength  $\lambda$  is most easily eliminated on a mesh of size  $\delta x \approx \lambda$  by a simple iterative method like Jacobi, Gauss-Seidel, or SOR, which is called as the *smoother*. In view of this, a hierarchy of grids with different mesh sizes is employed to numerically solve the finest grid problem. Transformations between different grid levels are required, that from the fine grid to the coarse grid is called as the *restriction* operator, and the *interpolation* operator means the transformation from the coarse grid to the fine grid. For more details on the multigrid method, see [14] and [15]. In the present computation, a multigrid V-cycle with a flexible number of grid levels is implemented with Successive-Over-Relaxation as the smoother. Injection and linear interpolation are used as the respective restriction and interpolation operators.

#### 4. PARALLEL IMPLEMENTATION

In order to achieve load balance and to exploit parallelism as much as possible, a general and portable parallel structure (Figure 2) based on domain decomposition techniques has been designed for the three dimensional flow domain. It has 1D, 2D and 3D partition features which can be chosen according to different geometry requirements. MPI is used for communications, which are required when subdomains on each processor need neighbors' boundary data information. The parallel computation is carried out

by executing the following sequence on each sub-domain with a communication procedure added at each iteration step for all flow fields:

1. Choose a domain decomposition structure by applying 1D, 2D, or 3D partition.
2. Guess the flow field at the initial time step including the velocity  $u, v, w$ , the temperature  $T$ , and the pressure field  $p$ .
3. Advance the flow to the next time step: update the coefficient  $b$ .
  4. Solve the temperature equation (19) using the multigrid method and exchange data information on partition interfaces.
  5. Evaluate the coefficients of the momentum equations and solve the velocity equations (11), (12), and (13) by the multigrid method and exchange data information on partition interfaces.
  6. Solve the pressure equation (18) by the multigrid method and exchange data information on partition interfaces.
  7. Correct the velocity and the pressure fields by using (14), (15), (16), and (17).
  8. Cycle 4 to 7 until convergence is achieved.
  9. Go to next time level and exchange data information on partition interfaces.
  10. Cycle 3 to 9 until convergence for a steady solution is achieved.

The parallel multigrid solver for the pressure equation is summarized as the following: For the pressure equation  $a_p b'_p = \sum_j a_{pj} b'_{jh} + b_p$ , the discrete form can be rewritten as  $A_p b'_p = b'_p$  at the mesh  $h$  level, here  $p'$ ,  $b'_p$  are simplified by  $P$ ,  $b$ , and  $A$  is the local coefficient matrix of the finite volume pressure equation. And the parallel V-Cycle scheme  $P^h \leftarrow M P^h (P^h, b^h)$  with total grid levels=  $N$  is outlined as :

1. Do  $k = 1, N - 1$
- Relax  $n_1$  times on  $A^h P^h = b^h$  with a given initial guess  $P_0^h$ , and after each relaxation iteration, exchange edge values with neighbors.
- $b^{2h} \leftarrow I_h^{2h} (b^h - A^h P^h)$ ,  $P^{2h} \leftarrow 0$
- Enddo
2.  $k = N$  (the coarsest grid , solve  $A^h P^h = b^h$
3. Do  $k = N - 1, 1$
- Correct  $P^h \leftarrow P^h + I_h^{2h} P^{2h}$ .
- Relax  $n_2$  times on  $A^h P^h = b^h$  with initial guess  $P_0^h$ , and after each

relaxation iteration, exchange edge values with neighbors.

Enddo

Here,  $I_h^{2h}$  and  $I_{2h}^h$  are restriction and interpolation operators, respectively, and in the present study, injection and linear interpolation are used. A similar multigrid scheme as above is used for the velocity and temperature equations. For low Rayleigh numbers, initial conditions throughout the flow domain, for example, can be set by  $T = x/L$ , and  $u = v = w = p = 0$  for computations. For high Rayleigh numbers, initial conditions can be generated from a steady flow at a lower Rayleigh number. The application is implemented on the Intel Paragon, the Cray T3D, T3E, the IBM SP2, and the Beowulf system with MPI as the message passing library, but it can be easily ported to other distributed memory systems with MPI software.

A brief description of the parallel computing systems used for the present study is given here.

The Intel Paragon XP/S at the Jet Propulsion Laboratory (JPL) is currently configured with 56 compute nodes, and each one has a peak speed of 75 MegafLOPS and 32 Megabytes memory. The one at the California Institute of Technology has 448 compute nodes. The operating system is the Paragon OS<sup>v</sup>/I, based on the OSF<sup>v</sup>/I operating system from the Open Software Foundation.

The Cray T3D at Goddard Space Flight Center, currently one of the most powerful MIMD computers available, has 512 compute nodes with 150 MegafLOPS peak performance and 64 Megabytes memory per node. Logically, it has a shared memory, and physically a distributed memory, associated with a processor.

The Cray T3E at NASA Ames is a 160-node MIMD parallel computer composed of IBM RS6000/590 workstations connected by a fast network. Each node has at least 128 Megabytes memory per node. The machine is expected to improve the performance of applications three to four times that of the T3D.

The IBM SP2 at NASA Ames is a 160-node MIMD parallel computer composed of IBM RS6000/590 workstations connected by a fast network. Each node has at least 128 Megabytes of main memory and 2 Gbytes of disk space. A maximum performance is 266 MegafLOPS each

node.

A typical Beowulf system, such as the machine at JPL, has 16 nodes interconnected by 100" base T Fast Ethernet. Each node may include a single Intel Pentium Pro 200 MHz microprocessor which has a peak speed of 200 MegaFLOPS, 128 Megabytes of DRAM, 2.5 Gbytes of IDE disk, and PCI bus backplane, and an assortment of other devices. It is a loosely coupled, distributed memory system, running message-passing parallel programs that do not assume a shared memory space across processors.

## 5. PARALLEL PERFORMANCE

In order to compare the performance on each system, 16 processors were used for the parallel code due to the current maximum number of nodes on the JPL Beowulf system. Here a model with  $R = 10^6$  and  $\sigma = 0.733$  in the unit cube with various mesh sizes was tested on those machines. The computation results are showed in Table 1, which lists the wallclock time at fixed time steps on the test problem for the five systems. The Cray T3E gives the best performance, and the IBM SP2 shows better performance than the Cray T3D, the Beowulf, and the Paragon. The difference of the time among those systems varies with grid sizes. For a small grid size like  $32 \times 32 \times 32$ , the communication is dominated. Hence, the discrepancy of the time for the entire computation on the five systems depends mainly on the difference of network connection. Once the grid size increases, the computation becomes dominated. Then the discrepancy of the time is more consistent with the difference of hardware. There is a big jump from grid size  $64 \times 64 \times 64$  to  $128 \times 128 \times 128$  on the Paragon, this is because the later grid is the largest size can be run on the JPL Paragon with a large amount of pageins. It is similar with the Beowulf system. Once the grid size reaches  $256 \times 256 \times 256$ , it could not be run efficiently because of the pageins. Usually for productive runs with certain number of processors used, those kind of grid sizes which surpass the system's memory size should be avoided. Once pageins are noticed, it is necessary to increase the number of processors.

The speedup measurements of the parallel code were carried out on the Cray T3E, T3D, and the Beowulf system. A grid size  $128 \times 128 \times 128$  with a test model of  $R = 10^6$  and  $\sigma = 0.733$  in

a cube for two time steps was used as our test problem. It has more than 10 million unknowns. Figure 3 shows the efficiency of the parallel code with different number of processors on the three systems. The lines are nearly linear on these systems, but on the Beowulf system the curve bends slightly when the number of processors increases. This is because the computation speed of the Beowulf node is faster than that of the Cray T3D node, but the communication speed on the Beowulf is slower than that of T3D and T3E. It is interesting to note that the results on Beowulf is better than that on T3D when processor number less than 8, but once the number increases, the T3D gives a better performance due to the fast communication network. Once a large number of processors is used, the communication part of the code is increased so a parallel system with a faster communication network gives a better result. The curves on T3E and T3D are very similar except the code on T3E runs about four times faster than that on T3D which is very consistent with the hardware's difference. From the present results, the code gives a very promising efficiency which should allow us to use a large number of processors with large grid size solving large scale flow problems in a three dimensional geometry.

In order to understand the efficiency of the parallel partitions, results with a model of the Rayleigh number  $10^6$ , the Prandtl number 0.733, and a grid size  $128 \times 128 \times 128$  have been obtained on the Beowulf on 16 processors by using different parallel partitions. In the Table 2, it shows the total wallclock time for a cube cavity at fixed time steps by using three types of partitions. It is obviously that for such a geometry with 16 processors, 3D partition has the best results as it minimized the communication. The present parallel structure allows us to use different partition to suit various physical domains.

## 6. NUMERICAL RESULTS AND DISCUSSION

Various numerical tests have been carried out for the 3D code. The results show that the numerical scheme is robust and reliable. Here numerical results of  $R = 14,660$  to  $10^7$ ,  $\sigma = 0.733$  in  $0 \leq r, u, z \leq 1$  are presented by the velocity and temperature fields. Grid sizes  $64 \times 64 \times 64$  for  $R = 14,660$  and  $128 \times 128 \times 128$  for  $R = 10^6$ ,  $10^7$  with 3D partition are used for the computation.

The results of  $R = 14,660$  are displayed in Figure 4. The velocity on the whole flow domain gives a complete picture of the three-dimensional flow. It is easy to see the flow rises from the hot side, travels horizontally, and sinks from the cold side. The flow principally remains in a single cell which is very similar to the two dimensional flow structure [4]. For  $R = 10^6$  in Figure 5, the flow structure becomes more interesting, and the flow is no longer a single circulation structure. The thin thermal boundary layers are formed on the two sidewalls. Large velocities ( $u, w$ ) appear near the side walls and the interior core is almost stagnant. The flow fields on the  $x - z$  plane at  $y = 0.5$  with the present range of Rayleigh number have similar flow patterns as those of the two dimensional cases [4].

Once the Rayleigh number increases to  $10^7$  in Figure 6, the velocity field becomes very complicated. Strong transverse flows are generated near the lower and upper corners, and the temperature field shows the very thin boundary layers on the two sidewalls and the near-linear temperature stratification in the interior. In the Figure 6(e), the detailed profile of the velocity near the lower corner shows that a separation of flow occurs on the bottom near the lower corner. It is interesting to compare the present results with that of the two dimensional case. Haldenwang [2] reported that regions of reverse flow on the horizontal walls are present for  $Ra \geq 10^{7.5}$  in two dimensional computations. The present three dimensional results show the separation at a lower Rayleigh number compared with the 2D case. For the Rayleigh number equal to  $10^7$ , the solution of 3D is no longer similar to the 2D case. It starts to show the significant difference of the flow features from the 2D solutions. 2D results are very useful to understand the flow structure in some extend, but the the 3D solutions give complete pictures of the flows which are more realistic and interesting.

Figure 7 shows the detailed profiles of the velocity component ( $v$ ) on  $x - y$  plane at fixed  $z$  values. Here the y-variations of the flows are appreciable, especially at the corners of the cavity the velocities vary rapidly and strong flow ( $v$ ) are generated over there. But the variations at the middle region are much less than those at the corner areas. Those flows affect the main streams gradually through the corners. In conclusion the flow is no longer a two dimensional motion with the increases of the Rayleigh

numbers, and the y-variations are not negligible. More numerical studies for three dimensional time-dependent flows with high Rayleigh numbers are under investigation.

## 7. CONCLUSIONS

In the present study, the finite volume method with an efficient and fast multigrid scheme has been implemented successfully to solve for three-dimensional, time-dependent, incompressible fluid flows on the Intel Paragon, the Cray T3D, T3E, the IBM SP2, and the Beowulf system through effective use of domain decomposition techniques. By various tests on the parallel systems and comparisons with some previous results, the parallel code shows very good convergence and efficiency on those systems, which indicate the potential capability for solving large complicated fluid dynamics problems on any distributed memory architectures which support MPI for communications. The present parallel code has a very flexible partition structure which can be used for any rectangular geometry by applying a 1D, 2D, or 3D partition to minimize communication. This feature allows us to study various thermal cavity flows with different geometries on parallel systems.

The comparison of wallclock time for fixed time steps among these systems gives very useful information about the speedup by using advanced hardware systems. The discrepancy of the time on these systems is due to the difference of hardware on each system and the network connection used. It shows a good agreement with these systems. The code scales very well on different system, and achieves an excellent performance of speedups with number of processors.

Numerical results are obtained for various Rayleigh numbers ranging from 14,660 to  $10^7$ . They give a complete description of the three dimensional flow. The flow field gradually changes to a multiple roll structure from a single flow circulation as the Rayleigh number increases. Very thin thermal boundary layers are formed on the two sidewalls, and regions of reverse flow on the horizontal walls are present for  $R \geq 10^7$ . The y-variations are very strong near the corners, and eventually affect the main flow with the increases of the Rayleigh numbers so the whole motion of the flow becomes three-dimensional. In spite of the difficulties associated with large Rayleigh number simulation, our present results

illustrated here clearly demonstrate the great potential for applying this approach to solving much higher Rayleigh number flow in realistic, three-dimensional geometries using parallel systems with large grid sizes. Much higher Rayleigh numbers computations and transient features of thermal convection in 3D are under investigation.

The research described in this paper was performed at the Jet Propulsion Laboratory, California Institute of Technology, under contract to the National Aeronautics and Space Administration. The Cray Supercomputers used in to produce the results in this paper were provided with funding from the NASA offices of Mission to Planet Earth, Aeronautics, and Space Science. The author would like to acknowledge Dr. Robert Ferraro in JPL for many valuable comments and suggestions, and Dr. Peggy Li in JPL for providing the Figure 6(b) by using a parallel visualization system for large data sets on the CrayT3D.

## References

- [1] G. de Vahl Davis and J. F. Jones. Natural convection in a square cavity: a comparison exercise. *Int. J. Numer. Methods in Fluids*, 3:227–248, 1983.
- [2] P. Haldenwang. Unsteady numerical simulation by Chebyshev spectral methods of natural convection at high Rayleigh number. In *Proc ASME Winter Annual Meeting*, volume 60, pages 45–51, Anaheim, California, 1986.
- [3] J. E. Drummond and S. A. Korpela. Natural convection in a shallow cavity. *J. Fluid Mech.*, 182:543–564, 1987.
- [4] P. Wang. *Thermal Convection in Shallow Laterally-Heated Cavities*. Ph.D. Dissertation, City University, London, 1993.
- [5] P. Wang and P. G. Daniels. Numerical solutions for the flow near the end of a shallow laterally heated cavity. *J. Eng. Math.*, 28:211–226, 1994.
- [6] G. D. Mallinson and de Vahl Davis. Three-dimensional natural convection in a box: A numerical study. *J. Fluid Mech.*, 83:1–31, 1977.
- [7] T. Fugei, J. M. Hyun, K. Kuwahara, and B. Farouk. A numerical study of three-dimensional natural convection in a differentially heated cubical enclosure. *Int. J. Heat Mass Transfer*, 34:1543–1557, 1991.
- [8] F. H. Harlow and J. E. Welch. Numerical calculations of time-dependent viscous incompressible flow of fluid with free surface. *Phys. Fluids*, 8: No.12 2182–2189, 1965.
- [9] A. J. Chorin. Numerical solution of navier-stokes equations. *Math. Comp.*, 22:745–762, 1968.
- [10] P. J. Roache. *Computational Fluid Dynamics*. Hermosa, Albuquerque, N. Mex., 1976.
- [11] S. V. Patankar and D. B. Spalding. A calculation procedure for heat, mass and momentum transfer in three-dimensional parabolic flows. *Int. J. Heat Mass Transfer*, 15:1787, 1972.
- [12] J. P. Doormaal and G. D. Raithby. Enhancements of the SIMPLE method for predicting incompressible fluid flows. *Int. J. Heat Transfer*, 7:147–156, 1984.
- [13] S. V. Patankar. *Numerical Heat Transfer and Fluid Flow*. Hemisphere, New York, 1980.
- [14] A. Brandt. Multi-level adaptive solutions to boundary-value problems. *Math. Comp.*, 31:333–390, 1977.
- [15] S. F. McCormick. *Multilevel Adaptive Methods for Partial Differential Equations*. Frontiers of Applied Mathematics, SIAM, Philadelphia, 1989.

| <i>Systems</i> | $32 \times 32 \times 32$ | $64 \times 64 \times 64$ | $128 \times 128 \times 128$ | $256 \times 256 \times 256$ |
|----------------|--------------------------|--------------------------|-----------------------------|-----------------------------|
| Intel Paragon  | 60                       | 181                      | 1275                        | 923                         |
| Beowulf        | 41                       | 100                      | 177                         | 3423                        |
| Cray T3D       | 18                       | 58                       | 117                         |                             |
| IBM SP2        | 12                       | 38                       | 95                          | 280                         |
| Cray T3E       | 4                        | 14                       | 32                          | 155                         |

Table 1: Wallclock times (seconds) using 16 processors on various parallel systems for the air with the Rayleigh number  $10^6$ .

| $dR = 10^6$      | $1D$ partitioning<br>( $1 \times 1 \times 1$ ) | $2D$ partitioning<br>( $4 \times 4 \times 1$ ) | $3D$ partitioning<br>( $-1 \times 2 \times 2$ ) |
|------------------|--|--|---|
| $\sigma = 0.733$ | 162  | 56   | 51  |
| one time step    | 1122   | 1122   | 1409  |
| ten time steps   | 5452   |  |   |

Table 2: The effect of parallel partitions on a cube domain(second)

## List of Figures

1. The staggered grid configurations for velocities, pressure, and temperature.
2. 1D, 2D, and 3D partitions on a flow domain for parallel systems.
3. Speed up of the parallel 3D code with a grid size  $128 \times 128 \times 128$  on the Cray T3E ( $\diamond$ ), the Cray T3D ( $\circ$ ), and the Beowulf system ( $\Delta$ ).
4. Numerical results for  $R = 14460$ , (a) velocity on the 3D domain, (b) velocity at  $y = 0.5$ , (c) temperature at  $y = 0.5$ .
5. Numerical results for  $R = 10^6$ , (a) velocity on the 3D domain, (b) velocity at  $y = 0.5$ , (c) temperature at  $y = 0.5$ .
6. Numerical results for  $R = 10^7$ , (a) velocity on the 3D domain, (b) temperature on the 3D domain, (c) velocity at  $y = 0.5$ , (d) temperature at  $y = 0.5$ , (e) velocity near the lower corner at  $y = 0.5$ .
7. The variations of the velocity component ( $v$ ) on the  $x - y$  plane at (a)  $z = 0.98$ , (b)  $z = 0.5$ , (c)  $z = 0.02$ .

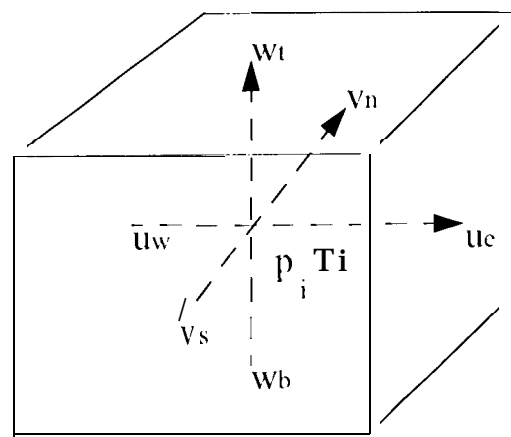


Fig. 1  
P. Wang

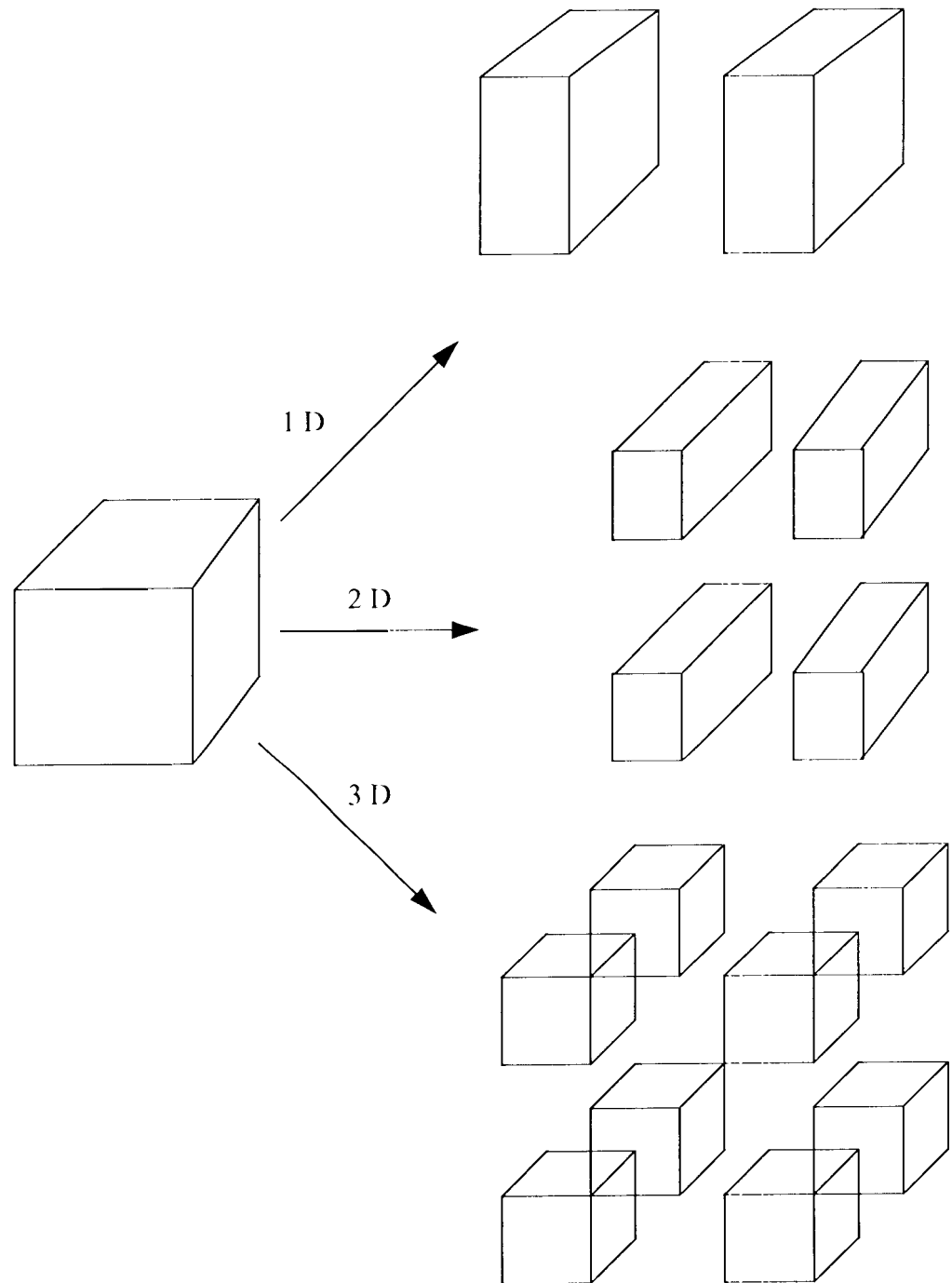


Fig. 2  
P. Wang

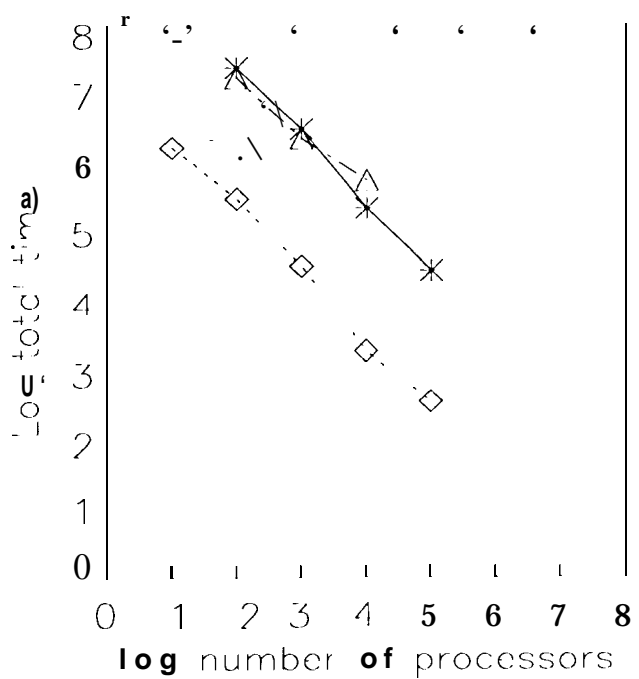
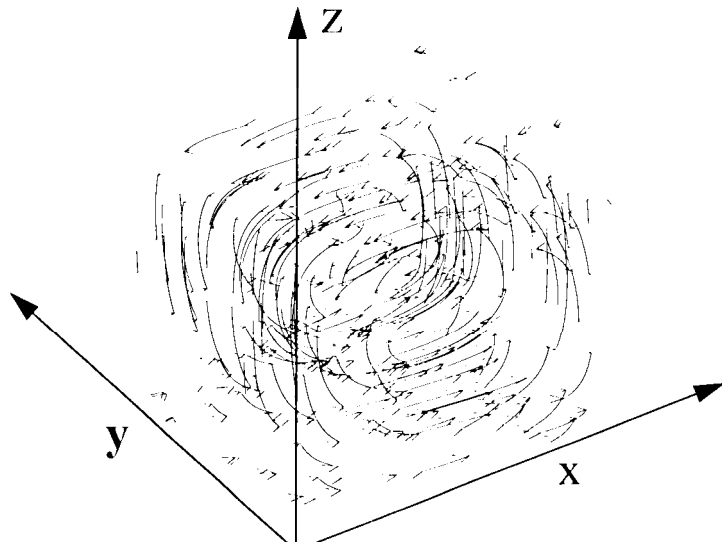
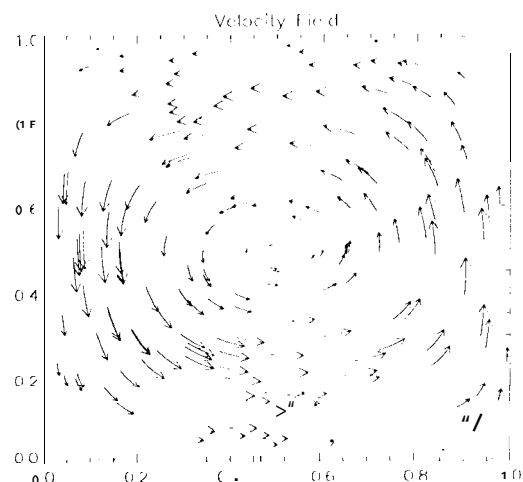


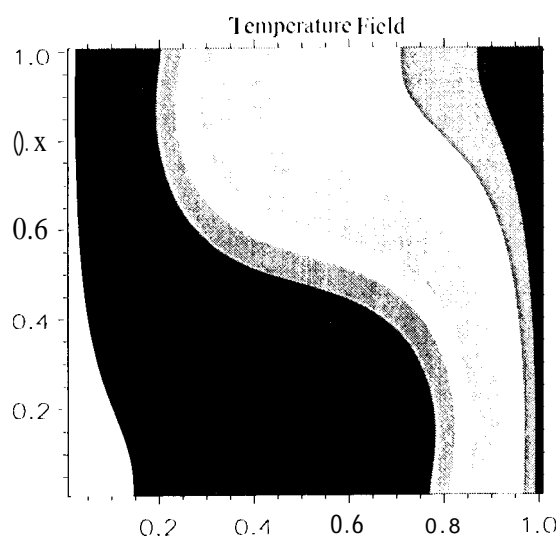
Fig. 3  
P. Wang



(a)

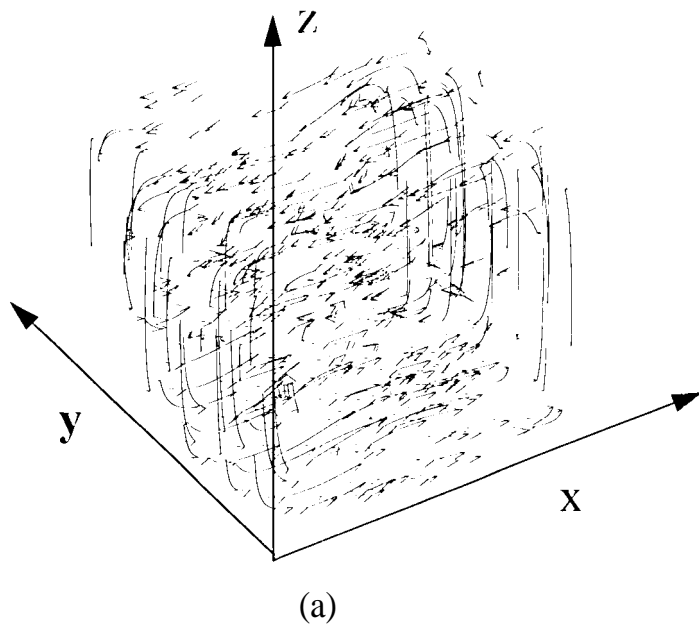


(b)

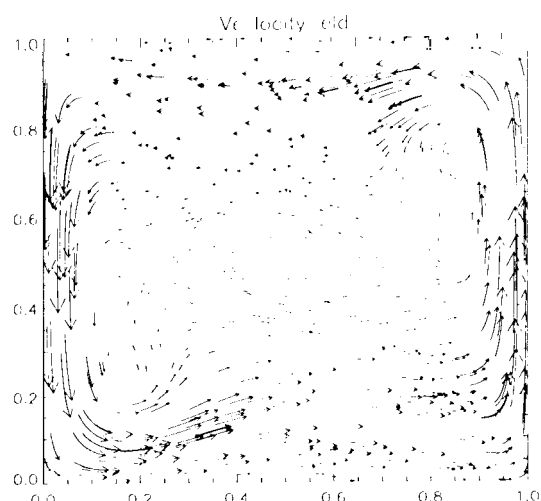


(c)

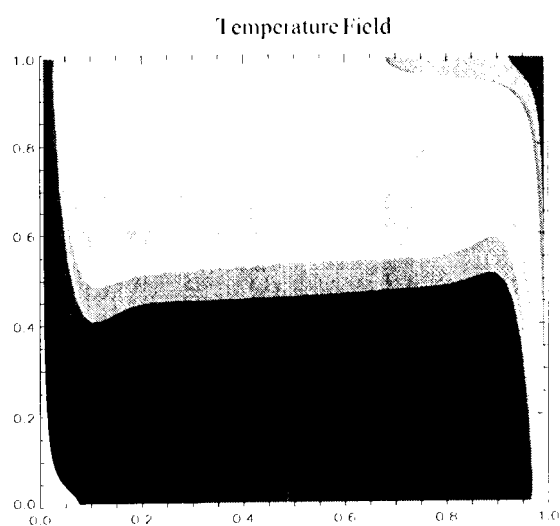
Fig. 4  
1'. Wang



(a)

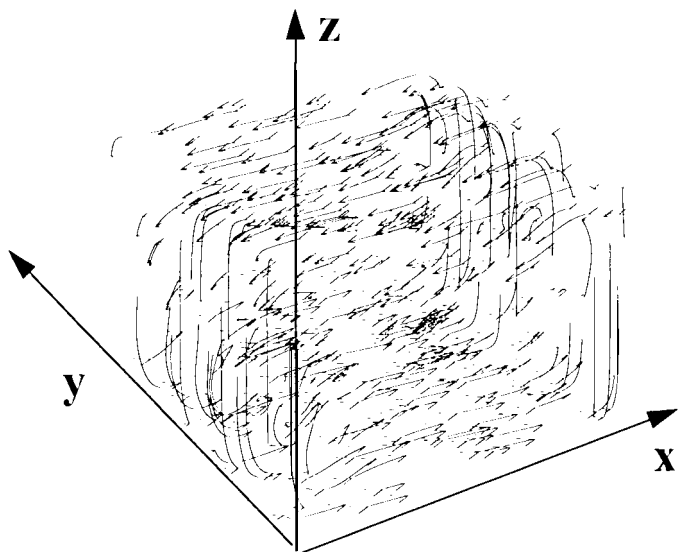


(b)

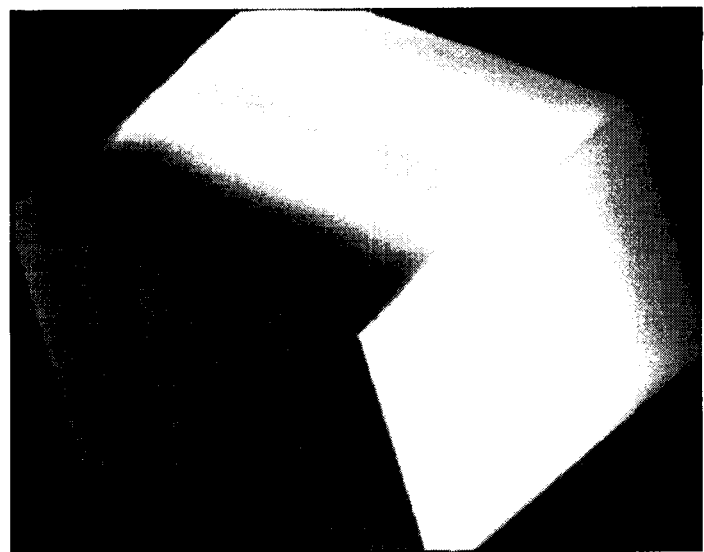


(c)

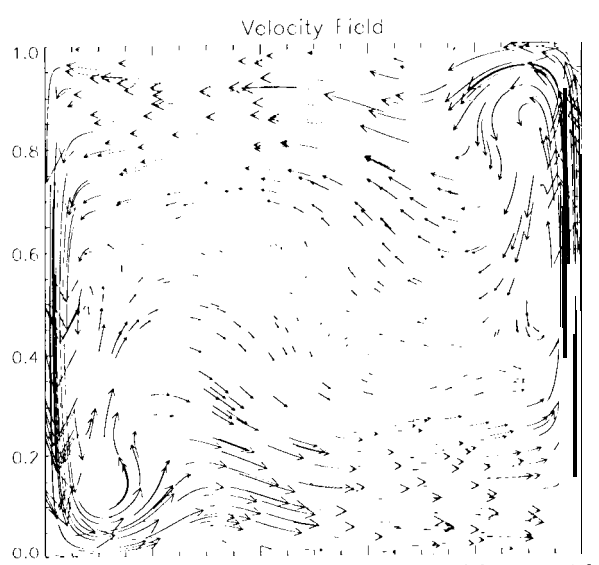
Fig. 5  
P. Wang



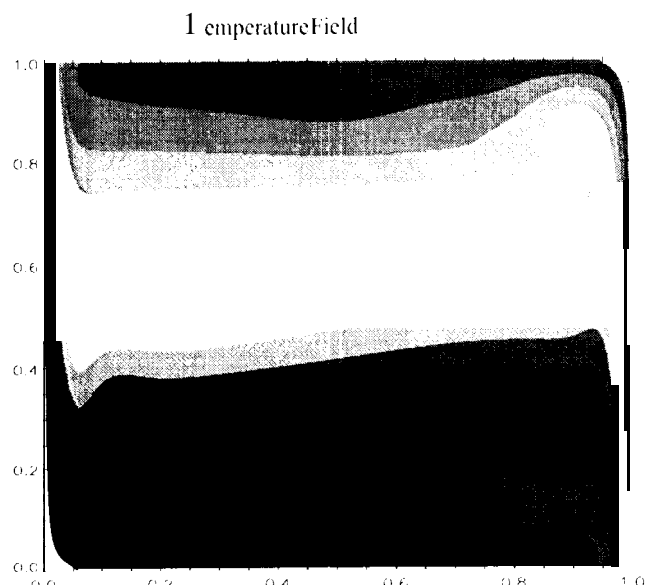
(a)



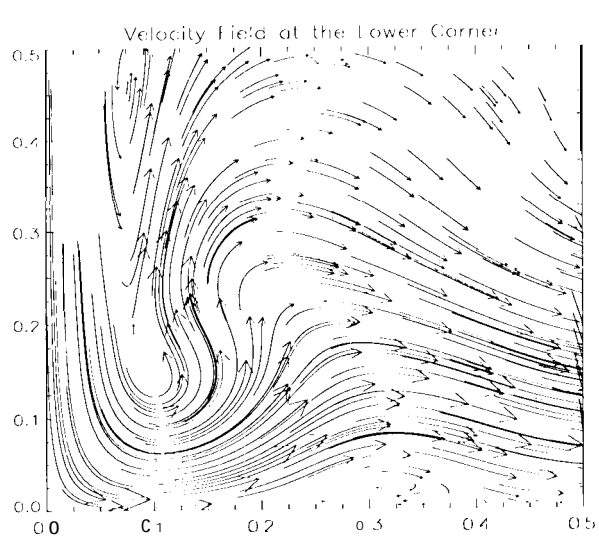
(b)



(c)



(d)



(c)

Fig. 6  
P. Wang

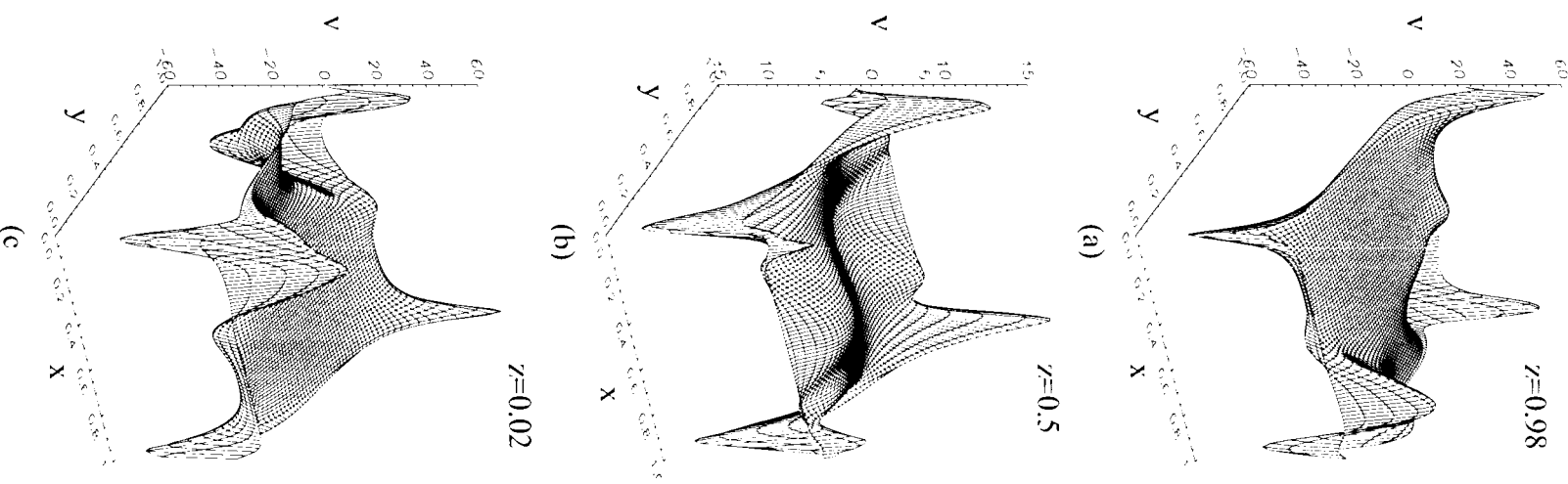
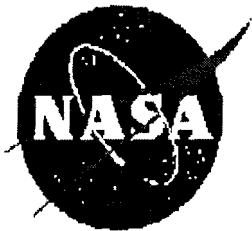


Fig. 7  
P. Wang



# 4th National Symposium on LARGE-Scale Analysis and Design on High-Performance Computers and Workstations

---

October 15-17, 1997 --> NOTICE TO AUTHORS

The Williamsburg Hospitality House, Williamsburg, VA

(Adjacent to Colonial Historic Area & College of William & Mary)

---



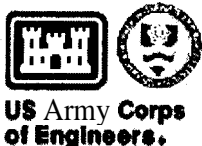
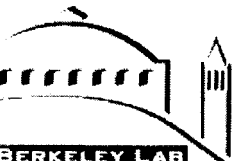
Sponsored by NASA Langley Research Center  
Hampton, VA

---



*Dr. John Malone's Welcome (LaRC Deputy Research Director)*  
in cooperation with





---

## Call for Papers <---

---

### Purpose and Emphasis

The NASA Symposium offers a unique opportunity for interactions between and among analysts (structures, electromagnetic and other disciplines) and developers of high- performance computers (**HPC**) and workstations.

We welcome your participation and encourage you to E-mail (plain text or postscript) 2-4 page abstracts and/or 1-page panel discussion proposals by May 15 in the following areas:

Development and/or Application of Efficient Algorithms for:

- Direct, iterative, (nonlinear, sequential/parallel equation solution
- Numerical Solution/Decomposition Methods and Load balancing
- Static, Dynamic, Thermal, Composite Structural Analysis
- Electromagnetic, Acoustic Heat Transfer and Flow Analysis
- Design-Optimization-Sensitivity (**Aeroelastic/interdisciplinary**)
- Efficient processor/memory use, Robustness, Portability & Scalability
- Software/programming/networking tools for seamless computing
- Large-scale applications of all types (Structures, **Electromagnetics** . ...)

Keynote Talk: John **C. Toole**, Director of the National **HPC** Coordination Office,  
Executive Office of the President  
Banquet Speaker: Gary **Smaby** (The **Smaby** Group)  
“The Future of HPC”

---



## Pre-Registration

Due to limited seating, attendees are encouraged to **pre-register**. This may be accomplished **by** completing the PRE-REGISTRATION FORM and returning it with a **\$200** check to NASA Langley no later than October 1st. The symposium **pre-registration** fee of \$200 covers the hardcover conference proceedings, reception, continental breakfast, refreshments during breaks, and special event. **Pre-registrants** (including NASA Langley employees covered **by** block registration) should pick up their registration packet, badge, symposium program and abstracts in the Hospitality House Ballroom after 1:00 PM, October 14th. Refunds will not be made for cancellations after the October 1st **pre-registration** deadline. Those who have not **pre-registered** **by** October 1st may register onsite for a fee of \$300.

## Accommodations

For the convenience of attendees, room reservations at the **Symposium** rate are available via a toll-free number 800-932-9192. A block of rooms has been reserved at the Symposium site, the Williamsburg Hospitality' House, 415 Richmond Road, Williamsburg, at a single/double guest room rate of \$76.00 plus 4.5 %state and 5 %city tax. Although our NASA block of rooms is already full, the Hospitality House is still accepting Symposium registrants at the same **low** rate until all their rooms are full. **THANKS WHH!** -----> specify NASA Symposium

<-----

This rate extends to stays before and after the Symposium (Ott 13 is a National Holiday), subject to availability. Reservations must be guaranteed with a major credit card.  
Register **NOW** at \$76 rate while rooms still last!

## Travel - Air Transportation (3 Airports)

Norfolk international Airport serves the Hampton Roads Area as well as Newport News/Williamsburg Airport. Norfolk is served by: American, United, Delta, USAir, Northwest, Continental, TWA, **Valujet**, Airtran, AirSouth, and Midway airlines. NN/W Airport is served **by**

**USAir** and **Valujet**. Richmond Airport is approximately 45 minutes north of Williamsburg on I-64.

## Local Transportation

Rental cars are not required as all Symposium functions will take place at the Hospitality House served **by** Airport limousines. Norfolk Air Shuttle (757-857-1231) offers Limo service from Norfolk Airport to Williamsburg (\$28 for 1 person or \$18 for 2-4). Williamsburg Shuttle (757-877-0279) offers **Limo** service to/from **NN/W** Airport (\$15 one way or \$27 round trip) and **to/from** Richmond Airport for \$50.

The Hospitality House is adjacent to the College of William and Mary and the Historic Colonial Capital. Two levels of Free Parking is available for guests in the basement of the Hospitality House.

## Check-in/Reception

The Hospitality House check-in time is 4 PM, however earlier **checkin** is possible **by** special request. After check-in, Symposium attendees and their guests are invited to register, get acquainted and mingle, take **the** Tour Bus to NASA or see a bit of Colonial Williamsburg. From 7-9 PM October 14th all Symposium attendees and spouses are invited to a reception, an excellent opportunity to renew old acquaintances and make new ones.

## Tour of NASA Langley Research Center

There are two opportunities (Tuesday and Friday) for attendees to have a FREE guided tour of NASA **Langley** Research Center. A Special Tour for Symposium attendees (NASA Bus) will leave the Hospitality house at Noon, Tuesday, Ott 14th., Proceed to the NASA main gate and NASA Langley getting off at several key stops to **go** in NASA facilities. At 2PM it will take attendees to the NASA **Langley** Colloquium **Lecture** in the Reid Center, and then return to the Williamsburg Hospitality House. Those arriving in Norfolk may drive their rental car to the NASA main gate by **2:30** where **they** can park and join the narrated tour & **Smaby** Colloquium (NASA is on the way to **Wmbg**). The Colloquium lecture may also **be** attended for FREE on Tuesday evening as part of the Sigma Series **Lectures** at 7PM at the Virginia Air and Space Museum. Featured Speaker at both is Gary **Smaby**, also our Symposium Banquet Speaker.

## Meals

**Historic** Colonial Williamsburg boasts many fine eating establishments as well as fast food restaurants within several blocks of the Hospitality House. Symposium attendees and spouses are invited to the Symposium reception at 7 PM on October 14th and the Symposium banquet at 7 PM on October 16th in the Berkeley Room. At the banquet, Mr. Gary **Smaby**, HPC Analyst with the **Smaby** Group will give an overview of the past, present and future of high-performance

computers and workstations. The **Reception**, Banquet, Continental Breakfast and refreshments at breaks and hardcover Symposium Proceedings are all included as part of the registration fee. If available, additional tickets **for spouses/guests to the special event must be purchased at the registration desk by noon on October 16th.**

## **Messages/FAX**

A message board is maintained in the Hospitality lounge outside the Berkeley Room. Participants may receive messages at (757)-229-4020. Information may be faxed to conference participants at (757)-229-9557.

## **Spouse's Activities**

Spouses are encouraged to visit some of the unique historical, cultural, scientific and shopping sites in the Hampton Roads area. These include **the** Virginia Air and Space Center, Colonial Williamsburg, Jamestown Colony, **Yorktown** Battlefields Visitor Center, the **Nauticus**, Williamsburg **Pottery**, Fort Monroe, Wells Theater, Chrysler Hall, MacArthur Museum, **Willet Hall**, Newport News Shipyard and boat tours. A special room for spouses near the registration desk is set aside for spouses to meet and make plans together. Both the Spouses room and the registration desk will have pamphlets listing the sightseeing and eating establishments in the area. Due to the close proximity to the sea, October weather in Williamsburg is often milder than elsewhere in the U. S.

## **Publications**

A Symposium program containing abstracts of papers to be presented will be available **by** May 1st on this **WWW** site and at registration. Plans are to provide registrants a hard-cover volume of proceedings (published **by Elsevier** Press) at registration. In addition, Symposium papers **will be** published in a special issue of the international Journal on Advances in Engineering **Software** Including Computing Systems in Engineering and available on the NASA Technical Report Server.

## **Presenters Information**

It is essential that all authors check the NASA Standards and Presentation Instructions for visuals (**Viewgraphs** are the preferred presentation medium) and Publication Instruction for Journal requirements. Speakers podiums are equipped with both stationary and roving microphones, a reading lamp and pointer.

Morning speakers are requested to arrive at the front of their presentation room with their visuals and meet with their Session Chair no **later** than **30** minutes prior to conference start time.

Afternoon speakers are asked to meet at the front of the Ballroom with their Session Chair prior to departing for lunch. Any questions concerning the Symposium Logistics should be addressed to

**Francine** Garner (7S7) 864-2907 or the **Technical** Chairman (757-864-2927). There is a 30-minute time limit (20 **for presentation**, 10 for introduction, questions and answers). Speakers should also meet with their Session Chair (or Co-chair) **for last-minute instructions prior to their** session.

# Symposium at a Glance

## Tuesday, Ott 14

- . 12:00 NASA Tour & Smaby lecture (2PM) - Bus from WHH (from Norfolk Airport, drive your rental car to NASA-on the way- and meet NASA Tour Bus at 12:30 at the NASA main gate)
- . 4:00 Return to Hospitality House from NASA via NASA bus
- . 1 :00+ hospitality House Checkin/Symposium Registration
- . 4:00 Exhibits
- 7:00 Reception

## Wednesday, Ott 15

- 7:30 Registration
- . 8:15 Welcome/Introduction (Doug Dwoyer, Director of Research, NASA Langley)
- . 8:30 Keynote Talk (John Toole, National HPCCP Office & NCSA)
- . 10:00 Session 1a: Structural Analysis -36,1,29,38 (Authors, Title & Affiliation below)
- . 10:00 Session 1b: Electromagnetics -7,8,34,24
- . 12:00 ----- 1,unch -----
- . 1:00 Session 2a: Structural Analysis -21,27,40
- 1:00 Session 2b: Flow Analysis -28, 22, 5
- 3:00 Session 3a: Solution Algorithms -9,18,32
- 3:00 Session 3b: Flow Analysis -25, 6, 15
- 4:00-----Exhibits -----
- . 5:00 Special Event (TBA) -----

## Thursday, Ott 16

- . 8:15 introduction (Woodrow Whitlow, Structures Division Chief, NASA Langley)
- . 8:30 Keynote Talk (Rattner/Scott, Intel)
- . 10:00 Session 4a: Finite Element Methods -10,4,43, 13
- . 10:00 Session 4b: Iterative Techniques -42, 30, 31, 12
- 12:00----- Lunch -----
- 1:00 Session 5a: Composite Structures -17, 14, 39
- . 1:00 Session 5b: Flow Analysis -26,37, 16
- 3:00 Session 6a: Nonlinear Methods -41, 11,33
- . 3:00 Session 6b: Analysis & Design -23, 35,3
- 4:00 Exhibits -----
- . 7:00 -----Banquet (included in Registration) ----- "HPC and Computer H/W and

**S/W now and in the Future” Speaker: Gary Smaby, Smaby Group**

## **Friday, Ott 17**

- . 8:15 - Keynote Talk (Bill Feireissen- NASA Ames): "HPC at NASA Now and in the Future"
- 9:15 Ahmed Noor - “Future Engineering Systems”
- 10:00 Session 7- “Panel of Experts”
- . 11:45 Best Paper Award (\$500 plus certificate)
- . 11:55 Closing Remarks
- . 2:00 2nd chance for Tour of NASA Langley (filling up fast??)

### **AUTHORS AFFILIATION TITLE**

1. M. Elgaaly and A. Seshasri - **Drexel University**  
Depicting the Behavior of Girders with Corrugated Webs **Up-to-Failure Using Non-Linear** Finite Element Analysis
3. S. N. Patnaik, R. M. Coroneos, 1). A. Hopkins Ohio Aerospace Institute& NASA Lewis  
Recent Advances in the Method of Forces: The Integrated Force Method of Structural Analysis
4. S. Yi - Nanyang Technological University, H. H. Hilton and M. F. Ahmad [University of Illinois at Urbana-Champaign] Viscoelastic Finite Element Analysis Algorithm Performance on **Course-Grained** and **Massively-Parallel** Supercomputers
5. X. Sun and Q. Hou: **Louisiana State University**  
A Three-Level Parallelization of Spatial Direct Numerical Simulation
6. V. N. Vatsa I). T. Hammond NASA **Langley, CSC**  
Viscous Flow Computations for Complex Geometries on Parallel Computers
7. A. Heirich J. Arvo Silicon Graphics& **Caltech**  
Parallel Radiometric image Synthesis
- 8.1'. Cwik J. Lou, D. Katz **JPL & Caltech**  
Scalable Finite Element Analysis of **Electromagnetic**
9. J. Qin D. Nguyen ODU A Tridiagonal Solver for **Massively Parallel** Computers
10. 1). Nguyen R. Qamar, 31. Runesha ODU  
Automatic Differentiation for Design Sensitivity Analysis of Structural Systems **Using** Parallel-Vector Processors
11. J. Manke, T. Wicks, I. Dadone, J. Hirsh and B. Oh - The Boeing Company  
Improved Rotor Tip-Relief Modeling by Coupling Comprehensive Rotor Analysis and Rotor Aerodynamics Code
12. V. Glinin Academy of Science of Ex-USSR  
Supercomputing - Yes, Supercomputer - No
13. D. F. Pilkey D. Inman, C. Ribbens Virginia Tech  
High-Performance Computing Issues for Model Reduction/Expansion
14. S. Yi Ling, Ying Nanyang Tec University, Singapore  
Finite Element Formulation for Composite Structures **with** Smart Constrained Layer Damping
15. F. Xiao and T. Ebisuzaki Computational Science laboratory, **RIKEN** Japan  
An Efficient Numerical Model for Multi-Phase Fluid Dynamics
16. M. Grismer W. Strnag, R. Tomaro & F. Whizeman Wright Patterson AFB  
Cobalt: A Parallel, implicit, [Unstructured Euler/Navier-Stokes Solver
17. K. Tamma R. Mohan University of Minnesota  
Advanced Manufacturing of Large Scale Composite Structures: Process Modeling, Manufacturing Simulations a
18. R. Kanapady M. Baddourah, K. Tamma University of Minnesota  
Domain Decomposition Computations **Using Vectorized Sparse Solver (VSS)** for Large Scale RTM Mold Filling S
21. W. Barry - Carnegie Mellon University, M. Jones (Virginia Tech) and P. Plassmann - Penn State University  
Parallel Adaptive Mesh Refinement Techniques for Plasticity problems
22. C. Riley and F. Cheatwood NASA **Langley**  
Distributed Memory Computing With the **Langley Aerothermodynamic Upwind** Relaxation Algorithm (LAURA)
23. A. Fijany T. Cagin, A. Jaramillo-Botero, S. Gulati, & W. Goddard **JPL**, California Institute of Technology  
Novel Algorithms for Massively Parallel, Long-Term, Simulation of Molecular Dynamics **Systems**
24. A. Statopoulos B. Rackner, Y. Saad, & J. Chelikowsky **University** of Minnesota  
Performance Optimization of Electronic Structure Codes on the **Cray T3E**

25. J. Sikora S. Ramakrishnan, L. LeBlanc Boeing  
Conversion of a Single Process **CFDCode** to Distributed and **Massively** Parallel Processing
26. W. Dai P. Woodward University of Minnesota  
Conservation **Laws** and Divergence-Free Condition in Three-dimensional Simulations for Supersonic **Magnetohydrodynamics**
27. D. Ghosh P. Basu Vanderplaats Research & Development, Inc.  
A Parallel Programming Environment for Adaptive P-Version Finite Element Analysis
28. P. Wang JPL  
Massively Parallel Finite Volume Computation of Three-dimensional Thermal **Convective Flows**
29. K. Kimsey S. Schramm, E. Hertel U.S. Army Research Lab  
Scalable Computations in Penetration Mechanics
30. G. Wang 1). Tafti NCSA-UIUC (II.)  
Uniprocessor Performance Enhancement with **Additive Schwarz Preconditioners** on Origin 2000
31. G. Wang 1). Tafti NCSA-UIUC (II.)  
Parallel **Performance** of Additive **Schwarz Preconditioners** on Origin 2000
32. H. Runesha D. Nguyen, A. Belegundu, '1'. Rchandrupatla ODU, Penn St, Rowen  
Interior Point Method and Indefinite Sparse Solver for **Linear Programming** Problems
33. N. Bouhmala Swiss institute of 'l'ethnology  
A parallel Simulated Annealing for Optimizing Mesh Partitions
34. X. Cai F. Yuan N.C. State [University]  
Stresses Around **Crack** Tip Due to **Electric Current** and Its Self-Induced **Magnetic Field**
35. 1). Katz T. Cwik, B. Kwan, J. Lou, P. Springer, '1'. Sterling, & P. Wang JPL & California Institute of Technology  
An Assessment of a **Beowulf** System for a Wide Class of Analysis and Design Software
36. R. Namburu Balsara, Bevins USCoE Waterways  
Advances in **Large-Scale Structural Mechanics** Explicit Calculations for Survivability and Protective Structures
37. D. Pepper D. Barrington, J. Lombardo University of Las Vegas  
A Parallel, h-Adaptive Finite Element Model for **Atmospheric Transport Prediction**
38. R. Chapman J. Cipolla, N. Nardacci Naval Undersea Warfare Center  
Two EBE Krylov Subspace Algorithms for Large-Scale 3-1) NAVY Applications
39. N. Rastogi S. Soni, A. Nagar AdTech Systems Research, Inc.  
Thermal Stresses in **Aluminum-To-Composite** Double-lap Bonded Joints
40. M. Ast R. Fischer, J. Labarta, & H. Manz INTES GmbH  
Run-Time Parallelization of Large FEM Analyses with PERMAS
41. K. Danielson R. Namburu USCoE Waterways  
Nonlinear Dynamic Finite Element Analysis on Parallel Computers Using FORTRAN 90 and **MPI**
42. M. Hayder D. Keyes, P. Mehrotra Institute for Computer Applications in Science and Engineering/NASA  
A Comparison of PETSc Library and HPF Directives for an ArchteypalPDE Computations
43. J. Sabu K. Heavey, E. Ferry U. S. Army Research Lab  
Computational Modeling of Multi-body Aerodynamic Interference
44. Panel M. Ginsberg G. Clifford, F. Felker, N. Lindsey, S. Shamsian, & S. Yunus HPC R&E, SGI/Cray, LSTC, H  
Panel: Future Directions for Commercial Finite Element Software

---

## Computer access

All guest rooms in the Hospitality House contain analog phone lines **where you can connect your notebook computer. In addition, there will be several Silicon Graphics (and perhaps SUN) workstations for use by Symposium attendees to check E-mail, etc.**



Dr. Olaf O. Storaasli  
Technical Chairman  
Mail Stop 240  
NASA Langley Research Center  
Hampton, VA 23681-0001  
757-864-2927 FAX : 757-864-8912  
Email: O.O. Storaasli@larc.nasa.gov

2/16/97

*a compressed PostScript version - Coming Soon!*

---

Computational Structures Branch